Photolithographically Manufactured Acrylate Multimode Optical Waveguide Translation and Rotation misalignment Tolerances

Hadi Baghsiahi[1], David R. Selviah, Guoyu Yu[2], Kai Wang, Michael Yau[3] and F. Aníbal Fernández
1-Department of Electronic & Electrical Engineering - University College London –
Torrington Place - London WC1E 7JE, 2-Optic Technium (OSL in North Wales), 3- Agilent Technologies Inc.
d.selviah@ee.ucl.ac.uk , h.baghsiahi@ee.ucl.ac.uk, k.wang@ee.ucl.ac.uk, a.fernandez@ee.ucl.ac.uk

Abstract

This paper reports numerous experimental measurements and modelling result of the loss caused by various amounts of translation and rotation misalignment in the optical backplane system. Combinations of VCSEL as the light source and waveguides of various widths have been input in the system. The source has been moved away from the centre of a channel waveguide in the horizontal and vertical direction gradually to find out the translation and rotation tolerance. Offsets between VCSEL-waveguide and waveguide-receiver have been studied to find the translation and rotation tolerance.

Introduction

Polymer optical waveguides fabricated on multilayer printed circuit boards can support 10 Gb/s data rates and higher without suffering from the bandwidth and electromagnetic interference (EMI)-limitations of conventional PCBs using only copper track interconnects [1]. For this technology to become widespread the cost must be minimised and the most costly parts are the input and output connectors [2]. Single mode waveguides have small core dimensions of typically 9 microns and so very precise active alignment in 6 axes (3 linear stages and 3 rotation stages) is required to align the socket to the waveguide and the plug to the optical source or detector. The socket and plug must be made to tight tolerances and designed to allow precise mating. In order to avoid these costly procedures and increase misalignment tolerance of a system, wider multimode waveguides are used in preference to single mode waveguide [3,4], and the waveguide cores are typically 50 – 100 microns. Even so the connectors have to be sufficiently well aligned to minimise possible misalignments along the 6 axes as these will cause additional loss [4].

In this paper a system of multimode waveguide backplane for storage area network is tested. The aim of the experiments and modelling is to find efficient and cost effective solutions to implement the system. Technically in this system, VCSELs are to be mounted on daughterboard while the backplane itself consists only of passive optical waveguides to increase its lifetime as the backplane is harder to replace than the daughterboard [5]. The daughterboard may experience vibration when plug in and out; other parts like hard disk or memory cards which are connected to backplane might vibrate or cause vibration in the entire system. So to have a robust system it is essential for the connector to be able to withstand relative misalignments within a certain tolerance.

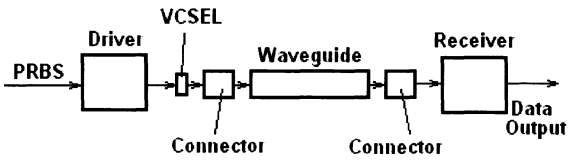

Fig. 1. Block diagram of optical backplane system.

A block diagram of an end-to-end single channel multimode optical backplane is shown in Fig (1). To assess the performance of this system, optical field generated from the VCSEL passed through the models of the functional blocks in the system. The coupling losses at VCSEL-waveguide and waveguide-receiver interfaces are investigated in this modelling to evaluate lateral and axial misalignment tolerance.

This paper is organized as follows. We describe the model of VCSEL, and also topics include Gaussian beam divergence, receiver and photo-detector's aperture that affecting system performance. Then we explained the modelling of multimode waveguide by using BPM technique. Finally, we present our experimental results and summary.

VCSEL

A. *Rate Equation*

VCSELs are one of the most important components in the system and it has complicated electrical, optical, and thermal characteristics that must be taken into consideration especially in theoretical modelling. As it has a very small cavity of about 1 μm length and several microns in lateral size, it will support typically one longitudinal mode and several transverse modes [6]. This spatial constitution determines other spatially dependent characteristics, such as spatial hole burning [7]. It is obvious that transverse mode profiles should be included in the modelling. The small cavity is prone to self-heating and consequently VCSEL will exhibit thermally-dependent behaviour [8]. Detailed analysis of VCSEL's spatial and thermal behaviour includes finite element method [9]. However, this method will consume much computation time and is not suitable for system level evaluation. Laser rate equations are well suitable for system level modelling [10]. The foundation of this spatially dependent equations are two coupled partial differential equations (PDEs) describing carrier and photon distribution [11].

B. *Spatial Profile*

Laguerre-Gaussian (LG) modes can be used to represent VCSEL's transverse mode distribution in a

cylindrical coordinate system [8]. The LG field profile is given by:

$$E_{ml} = \alpha_{ml} \cdot \left(\frac{\sqrt{2}r}{w_0}\right)^{l} \cdot L_m^l\left(\frac{2r^2}{w_0^2}\right) \cdot e^{-2(r/\omega_0)^2} \quad (7)$$

We modelled the VCSELs having up to four transverse modes. In table (1), a list of intensity of each mode we have used is shown [12]. Fig. 2 shows VCSEL outputs of these combinations.

TABLE (1): VCSEL OUTPUT MODE FIELDS INTENSITY DISTRIBUTION

Modes	Power Distribution			
1	1			
2	0.5		0.5	
3	0.125	0.75		0.125
4	0.06	0.44	0.44	0.06

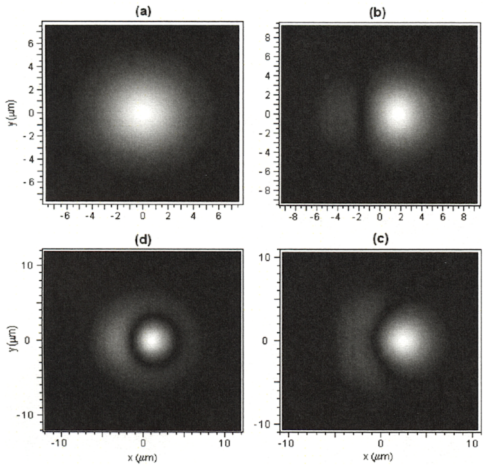

Fig. 2. Weighted VCSEL output field containing (a) one mode, (b) two modes, (c) three modes and (d) four modes.

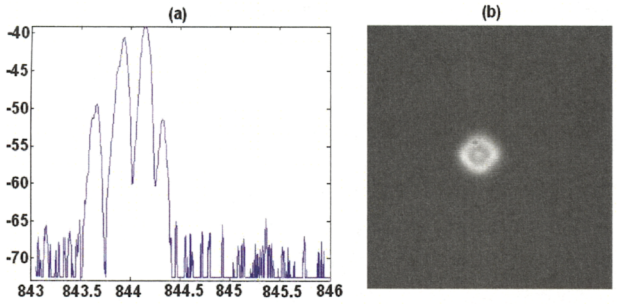

Fig. 3. Measured wavelength spectrum of a 10 Gbits/s VCSEL and a photograph of output field of a VCSEL from ULM photonics.

In figure (3) the field of a 10 Gbits/s VCSEL measured by a wavelength spectrum analyzer through a single mode fibre is shown. At driving current of 2.5 mA, four modes are clearly seen with middle two modes dominate power weighting. The spectrum spacing between second and first mode, third and second mode, fourth and third mode are 0.27nm, 0.22nm and 0.17nm respectively.

C. *Receiver Size*

The receiver's photodiode diameter is another important parameter to determine the misalignment tolerance [13]. In fig (5.a), a Gaussian beam of diameter 3.1 μm emits into a waveguide of core size 50 μm × 50 μm. At output end of waveguide, we can notice the optical field pattern due to modal interference. From this figure, we can understand that the power reading will vary with different receiver position relative to the waveguide core. Fig (5.b) shows an output from a waveguide of the same size by modelling. The difference of the pattern is due to the fact that these two outputs are taken from different length of waveguide. With the random nature of intensity distribution, it is difficult to optimum the position for receiving maximum power. In this respect, a larger-aperture receiver not only have the benefit of a better receiving power, but also a more stable power reading due to the averaging effect.

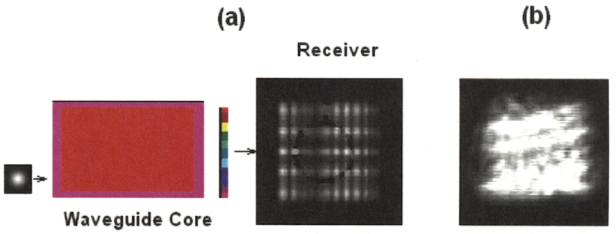

Fig5. (a) Modelling result of waveguide output with guide core size of 50 x 50 micron. (b) A photograph taken from waveguide output

Multimode waveguide and modelling

The modelling process is as follows. First, individual models of the components are set up. At the next step Beam Propagation Method (BPM) is used to determine the power loss due to axial and lateral misalignment and power distribution at the output end of waveguide. The Optical field of a VCSEL is sent through a single mode fibre. We modelled this single mode fibre to have the same situation as the experiment. The output field of the single mode was guided to the multimode channel waveguides at different widths. System power is verified to derive the translation and rotation tolerance.

The refractive index of the multimode channel waveguide is 1.526 for cladding and 1.556 for core area. The applied wavelength is 850 nm. As we have stated before, the VCSEL can operate in single mode or multimode state depends on operating conditions such as driving current intensity and temperature. A single-mode VCSEL will have a beam waist of 1.5 μm and a divergence angle of 20°. However, if a VCSEL has four transverse modes it will have a beam waist of 3 μm. The third step is to create the circuit. The waveguide has a square core which is surrounded by cladding material. In the front end of waveguide, an air gap has been varied from 0 to 1000 μm. The launching field was placed in front of waveguide separated by the air gap. The waveguide is2 mm long since it has been tested that the power in the guide remains constant after this length. Convergence test has been carried out on the selection of cross section step dx and dy and longitudinal step dz. Starting from dx=dy=0.1 μm dz=1 μm, it has been discovered that dx=dy=0.2 μm and dz=6 μm gave the same field distribution at output end of waveguide as the original steps. After the selection of above parameters, the

launch field is swept across the waveguide simulating the misalignments between VCSEL and waveguide. The launching field is first swept laterally from x=-50 μm to 50 μm with a step of 4 μm. (x is in the horizontal direction). Then the field is moved longitudinally 100 μm away from waveguide and performs the lateral sweep as before. This action finishes at z=1000 μm.

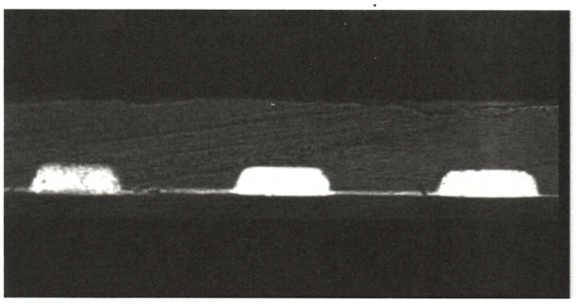

Fig: 4. Waveguide cross section showing guide of width 100, 110 and 120 μm.

EXPERIMENT AND RESULTS

D. *Translation tolerance*

Experiments are carried out regarding translation and rotation tolerance between a VCSEL and a straight waveguide. The set-up of the experiment is shown in fig (5). A six-axis stage was built by mounting three linear translation stages, one rotation stage and two tilt stages together. This six-axis stage is used to align optical source to waveguide and offset the source to waveguides to test translation tolerance between them.

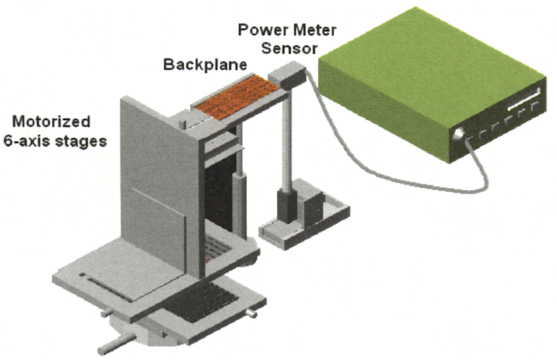

Fig 5. Diagram of experimental set-up.

First, the alignment was carried out with the help of visible light. After achieving a good alignment to a waveguide centre, the source is moved to the one side of the waveguide. Then, it was moved step by step towards waveguide core and the output power of waveguide is recorded. The scan was designed to finish at some place of other end of waveguide core. The source is then moved away from waveguide, going back to original lateral place and start to scan again. The whole process consists of ten of such iterations.

The result is meshed where values along *x* axis represent lateral misalignment between optical source and waveguide core centre. Values along *z* axis represent axial misalignment between optical source and waveguide. Fig 6. shows the modelled result (a) and experimental result (b). The waveguide width used in this figure is 50×50 μm.

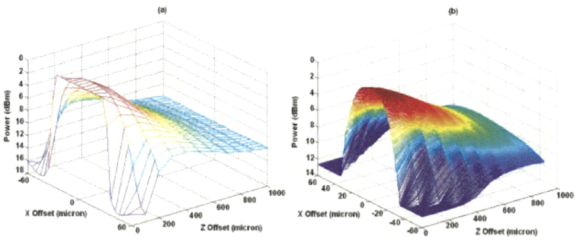

Fig 6. Output power with related to lateral and axial misalignment between VCSEL and waveguide. (a) Modelled result. (b) Experimental result.

A continuous scan of this translation tolerance test are carried out regarding different guide width of 10, 20, 30…100 μm. Considering a coupling tolerance of 0.5 dB on each connection between VCSEL-waveguide and waveguide-photodetector, a total 1 dB contour give an indication of lateral and axial tolerance, as shown in fig(7).

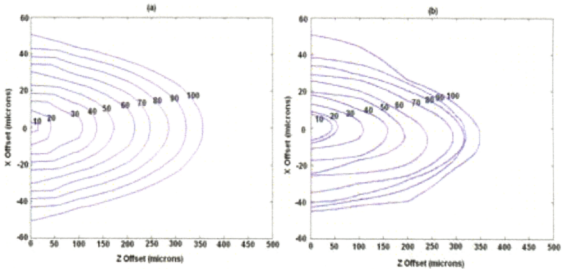

Fig. 7. Contour of 1dB of waveguides output power with related to misalignments. (a) Modelled result. (b) Experimental result.

With the confirmation of the above modelling result, further modelling work has been carried out on various conditions of VCSEL-the divergence angle can be 12° to 20°. The number of modes in a VCSEL could be up to 4 modes. In fig (8), some of the conditions have been adopted in the modelling. In each modelling, guide width various from 10 μm to 100 μm.

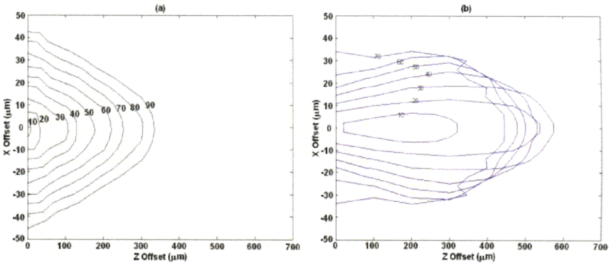

Fig. 8. Modelled results showing different coupling condition. (a) VCSEL divergence angle equals to 20 degree. (b) VCSEL divergence angle equals to 20 degree.

E. *Rotation tolerance*

A different experimental set-up is used for rotation tolerance test. This is due to the fact that the end of the source does not pass through the vertical axis of the 6-axis stage. This can cause problem since the rotation of the source along the vertical stage axis will bring about translation of the source to corresponding waveguide,

thus result in the total misalignment of source and waveguide considering the size of the waveguide. For the set-up of rotation tolerance test, as shown in fig (10), another rotation stage is used. A post is fixed onto it and these two share the same vertical axis. Part of the top of the post is engraved to produce the proximity between source and waveguide. A 2 mm gap is left in case the edge of the post touching the board at some rotation angle. The source is fixed in this case while the alignment of source and waveguide is performed using the 6-axis stage which carrying the board. At last, the sensor of power meter is aligned to the output of waveguide. The rotation and power reading is program controlled as before.

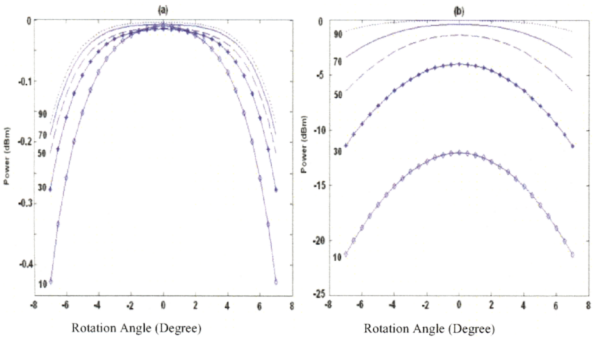

Fig. 9. Modelled results shows rotation tolerance at different guide width and the axial distance between source and waveguide is (a) zero and (b) 200 μm.

The results are compared in fig (11); (a) shows modelled result of rotation tolerance when axial distance is 200 μm between source and waveguide. (b) Represents experimental measurement corresponding to the modelling. Since a single mode fibre is used to perform the test, the maximum power level is -18.5 dBm. The graphs in (b) have been normalized to compare with modelling result. We can notice that these two results match well when guide width is 30, 50, 70 and 90 μm. for waveguide of 10 μm, since there is a power difference even at maximum position; the power readings have reached the meter's lowest detectable level at some rotation angle.

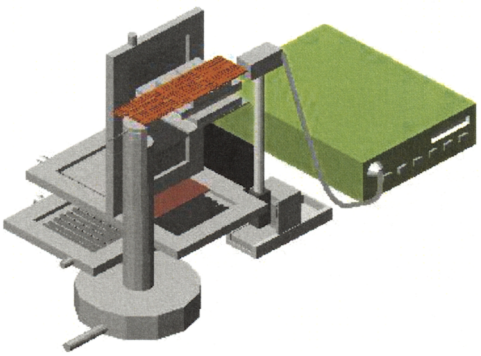

Fig. 10. Experimental set-up of rotation tolerance test.

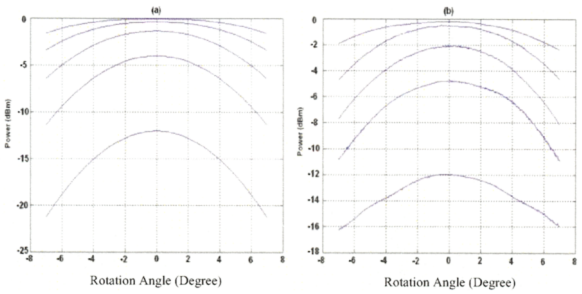

Fig. 11. Comparison of (a) modelled result and (b) experimental result of rotation tolerance of different guide width.

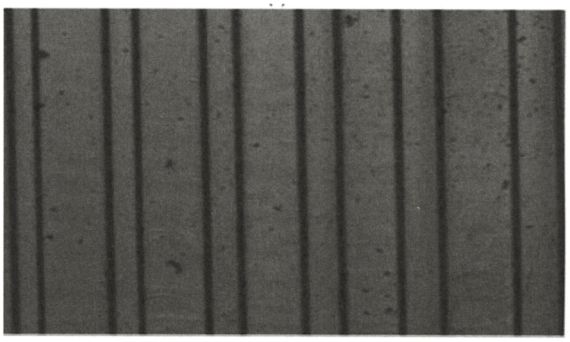

Fig. 12. Fabricated straight waveguide of 30, 40, 50, 60, 70 and 80 μm.

Acknowledgments

The authors would like to thank Dorothy Hodgkin Postgraduate Awards, IeMRC, and EPSRC for providing financial support to the project. Our industry cooperator-Xyratex has given their support through weekly talks.

References

1. Selviah, D. R, Fernández, A, Papakonstantinou, I.,Wang, K., Baghsiahi, H, Walker, A, McCarthy, A, H. Suyal, Hutt, D, Conway, D, Chappell, J, Zakariyah, S, Milward, D, "Integrated Optical and Electronic Interconnect Printed Circuit Board Manufacturing". *Circuit World* 34(2), 21-26, 2008
2. Yu, Guoyu, Selviah, D. R, "Modelling of optical coupling to multimode polymer waveguides: Axial and lateral misalignment tolerance," Accepted by 17th *Annual IEEE/LEOS Meeting*, Puerto Rico, 2004.
   Papakonstantinou,I., Selviah, D. R., Pitwon, R. A., Milward, D. "Low cost, precision, self-alignment technique for coupling laser and photodiode arrays to waveguide arrays". *IEEE Transactions on Advanced Packaging* . 2008.
4. Papakonstantinou, I, Selviah, D. R., Wang K., Fernandez. "Transition, radiation and propagation loss in polymer multimode waveguide bends". *Optics Express* 15(2), 669-679, 2007.
5. Rashed, A. M., Selviah, David R. "Source misalignment in multimode polymer tapered waveguides for optical backplanes". *Optical Engineering* 46(1), 015401(1)-015401(7), 2007.
6. Iga, K,"Surface-emitting laser-its birth and generation of new optoelectronics field," *IEEE J. Select. Topics Quantum Electron.* Vol. 6, No. 6, pp. 1201-1215, Nov. 2000.
7. Valle, A, Sarma J., Shore, K, "Spatial hole burning effect on the dynamics of vertical cavity surface-

emitting laser diodes," IEEE. J. Quantum Electron., vol. 17, no. 12, pp. 1423-1431, Dec 1995.
8. Hasnain,G., Tai, K., Yang, L, Fischer, Wynn, J. D., Weir, Dutta N. K. and Cho, "Performance of gain-guided surface emitting lasers with semiconductor distributed Bragg reflectors," *IEEE J. Quantum Electron.*, vol. 27, pp. 1377-1385, June 1991.
9. Hadley G. R, Lear K. L., Warren, Choquette, Scott, W., Corzine, "Comprehensive numerical modelling of vertical-cavity surface-emitting lasers," *IEEE J. Quantum Electron.*, vol. 32, pp. 607-616, Apr. 1996.
10. Jungo, M., Erni D., and Baechtold, "2-D VCSEL model for investigation of dynamic fiber coupling and spatially filtered noise," *J. Lightwave Technol.*, vol. 15, pp. 3-5, 2003.
11. Zeeb, Moller, Reiner G., Hackbarth T., and Ebeling, "Planar proton implanted VCSELs and fiber-coupled 2-D VCSEL arrays," *IEEE J. Selected* , vol. 1, no. 2, pp. 616-623.
12. "Spectral characterization of multimode laser diodes", TIA/EIA fibre optic tests procedure (FOTP) 127, 1991.
13. "Monolithic Integrated SiGe Optical Receiver and Detector". Paul C. P., Chen, Anand M. Pappu, Alyssa Apsel, B., Optical Society of America, *Integrated optoelectronic circuits*; (040.5160) 2007.